Molecular Biology of the Cell
Vol. 13, 2795–2809, August 2002

Function of Dynein and Dynactin in Herpes Simplex Virus Capsid Transport

Katinka Döhner,* André Wolfstein,* Ute Prank,* Christophe Echeverri,† Denis Dujardin,† Richard Vallee,† and Beate Sodeik*‡

*Institute of Biochemistry, Hannover Medical School, Hannover D-30623, Germany; and †Department of Pathology, Columbia University, New York, NY 10032-3702

Submitted July 13, 2001; Revised May 21, 2002; Accepted June 5, 2002
Monitoring Editor: Lawrence S. Goldstein

After fusion of the viral envelope with the plasma membrane, herpes simplex virus type 1 (HSV1) capsids are transported along microtubules (MTs) from the cell periphery to the nucleus. The motor ATPase cytoplasmic dynein and its multisubunit cofactor dynactin mediate most transport processes directed toward the minus-ends of MTs. Immunofluorescence microscopy experiments demonstrated that HSV1 capsids colocalized with cytoplasmic dynein and dynactin. We blocked the function of dynein by overexpressing the dynactin subunit dynamitin, which leads to the disruption of the dynactin complex. We then infected such cells with HSV1 and measured the efficiency of particle binding, virus entry, capsid transport to the nucleus, and the expression of immediate-early viral genes. High concentrations of dynamitin and dynamitin-GFP reduced the number of viral capsids transported to the nucleus. Moreover, viral protein synthesis was inhibited, whereas virus binding to the plasma membrane, its internalization, and the organization of the MT network were not affected. We concluded that incoming HSV1 capsids are propelled along MTs by dynein and that dynein and dynactin are required for efficient viral capsid transport to the nucleus.

INTRODUCTION

To initiate a successful infection, animal viruses bind to the cell surface, penetrate into the cytosol, and target their genome to the sites of viral transcription and replication. For many viruses this is the host nucleus (Whittaker *et al.*, 2000). Particular neurotropic viruses that enter at the presynaptic plasma membrane, such as herpes simplex viruses, are transported over long distances because the site of entry is far away from the nucleus. Herpes simplex virus type 1 (HSV1) is a human pathogen that initially replicates in epithelial cells of the oral cavity. Amplified virus enters neurons and is transported to the neuronal nuclei located in the trigeminal ganglion (reviewed in Enquist *et al.*, 1998). After lytic infection of some neurons, a latent infection is established (Wagner and Bloom, 1997).

Article published online ahead of print. Mol. Biol. Cell 10.1091/mbc.01–07–0348. Article and publication date are at www.molbiolcell.org/cgi/doi/10.1091/mbc.01–07–0348.

‡ Corresponding author. E-mail address: Sodeik.Beate@MH-Hannover.de.

Abbreviations used: DHC, dynein heavy chain; DIC, dynein intermediate chain; HSV1, herpes simplex virus type 1; gX, viral glycoprotein X; GFP, green fluorescent protein; mAb, monoclonal antibody; MOI, multiplicity of infection; MT, microtubule; MTOC, MT organizing center; pAb, polyclonal antibody; PFU, plaque-forming units.

We have calculated that it would take 231 years for a herpes virus capsid to diffuse by 10 mm in the axonal cytoplasm (Sodeik, 2000). High concentrations of protein, the cytoskeleton, and organelles cause molecular crowding in the cytoplasm, which effectively restricts free diffusion of molecules larger than 500 kDa (Luby-Phelps, 2000). Thus, virions and subviral particles are transported by active processes. Besides hijacking vesicular transport during endocytosis and secretion, viruses also exploit the host's cytoskeleton directly for their itinerary (Sodeik, 2000; Ploubidou and Way, 2001).

HSV1 virions consist of four structural components: DNA, capsid, tegument, and envelope (Steven and Spear, 1997; Zhou *et al.*, 2000). The icosahedral capsid with a diameter of 125 nm surrounds the double-stranded viral DNA of 152 kb. The tegument, the hallmark of all herpes viruses, is an amorphous layer of ~20 proteins. It is localized between the capsid and the viral envelope that contains ~12 membrane proteins.

For cell entry the envelope of HSV1 fuses with the plasma membrane. Different molecules such as heparan sulfate proteoglycans, members of the tumor necrosis receptor family (HVEM), and the immunoglobulin family (nectins) serve as receptors for the HSV1 viral glycoproteins gB, gC, and most importantly gD (reviewed in Spear *et al.*, 2000). The fusion of the viral envelope with the plasma membrane is mediated by the viral glycoproteins gB, gD, gH, and gL (Spear *et al.*, 2000).

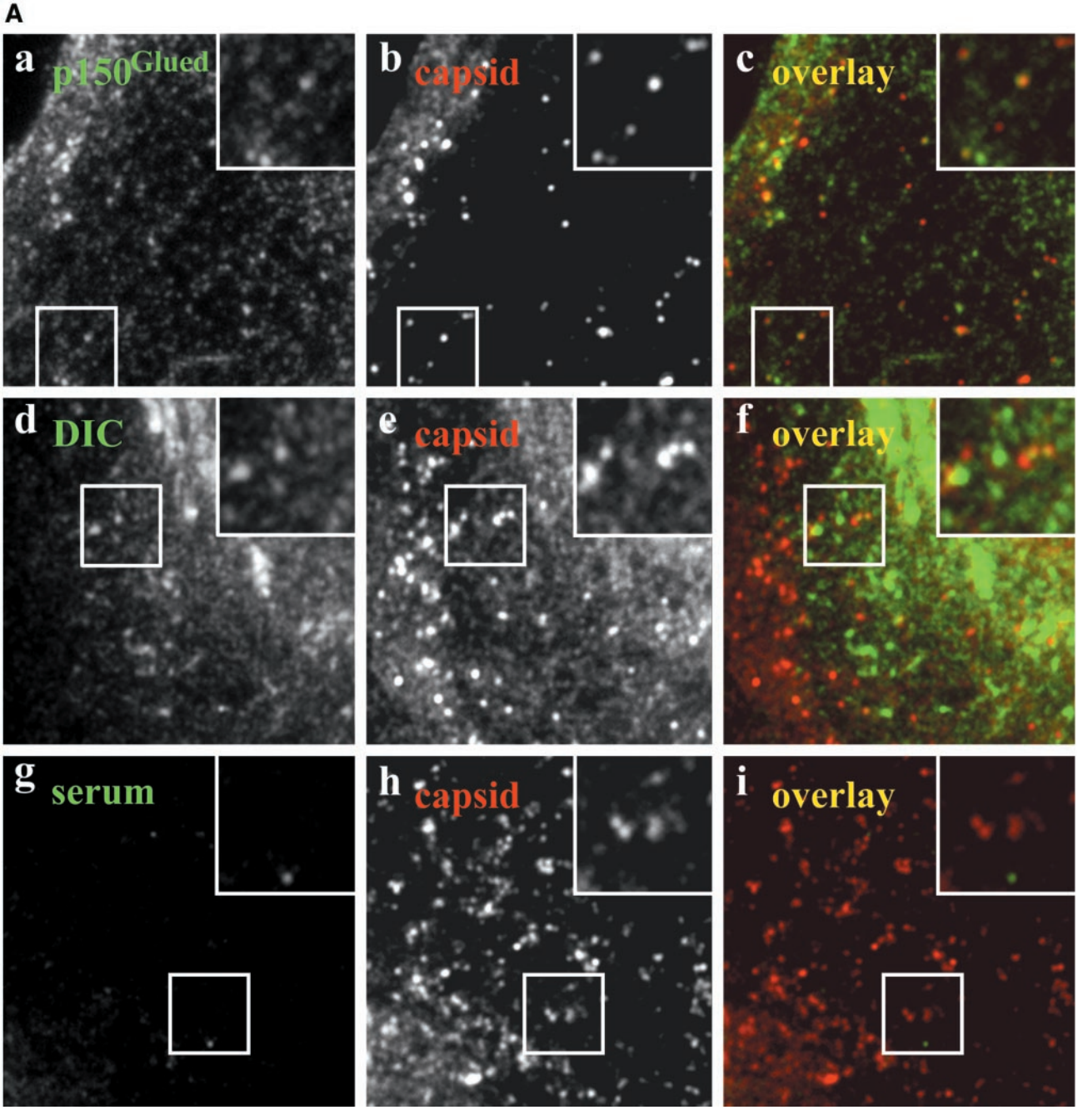

Figure 1. (A) Incoming wild-type HSV1 capsids colocalize with p150^{Glued} and DIC. A significant fraction of incoming HSV1 capsids colocalizes with p150^{Glued} and DIC (yellow dots in the overlays, c and f). This apparent colocalization is not due to binding of rabbit IgG to the herpes virus Fc receptor on the surface of infected cells because there is no signal from a nonimmune rabbit serum (i). Moreover, immunoblots confirmed that there is no unspecific cross-reactivity of the anti-dynactin or anti-dynein antibodies to structural viral proteins (our unpublished results). Immunofluorescence microscopy of PtK_2 cells infected with wild-type HSV1 for 1 h in the presence of 0.5 mM cycloheximide. Cells were fixed with PHEMO-fix at room temperature, blocked with 0.2 mg/ml pooled human IgG and 5 mg/ml BSA and double-labeled with anti-p150^{Glued} (pAb Portos; a), anti-DIC (pAb L5, d) or a nonimmune rabbit serum (serum, g) and anti-VP5 (mAb 5C10; b, e, and h). Note, that the anti-VP5 antibodies cross-reacted in PtK_2 cells weakly with the cortical actin and stress fibers. (B) Incoming HSV1 capsids of a gE deletion mutant colocalize with p150^{Glued} and DIC. Incoming HSV1 capsids of the mutant strain R7202 that does not express a viral Fc receptor colocalize with p150^{Glued} and DIC (yellow dots in the overlays, c and f). Moreover, there is no colocalization (i) after double labeling with a nonimmune rabbit serum (g) and capsid antibodies (h). Immunofluorescence microscopy of PtK_2 cells infected with HSV1 deleted for gE (R7202) for 1 h in the presence of 0.5 mM cycloheximide. Cells were fixed with PHEMO-fix at room temperature, blocked with 0.2 mg/ml pooled human IgG and 5 mg/ml BSA and double-labeled with anti-p150^{Glued} (pAb Portos; a), anti-DIC (pAb L5, d), or a nonimmune rabbit serum (g) and anti-VP5 (mAb 5C10; b, e, and h).

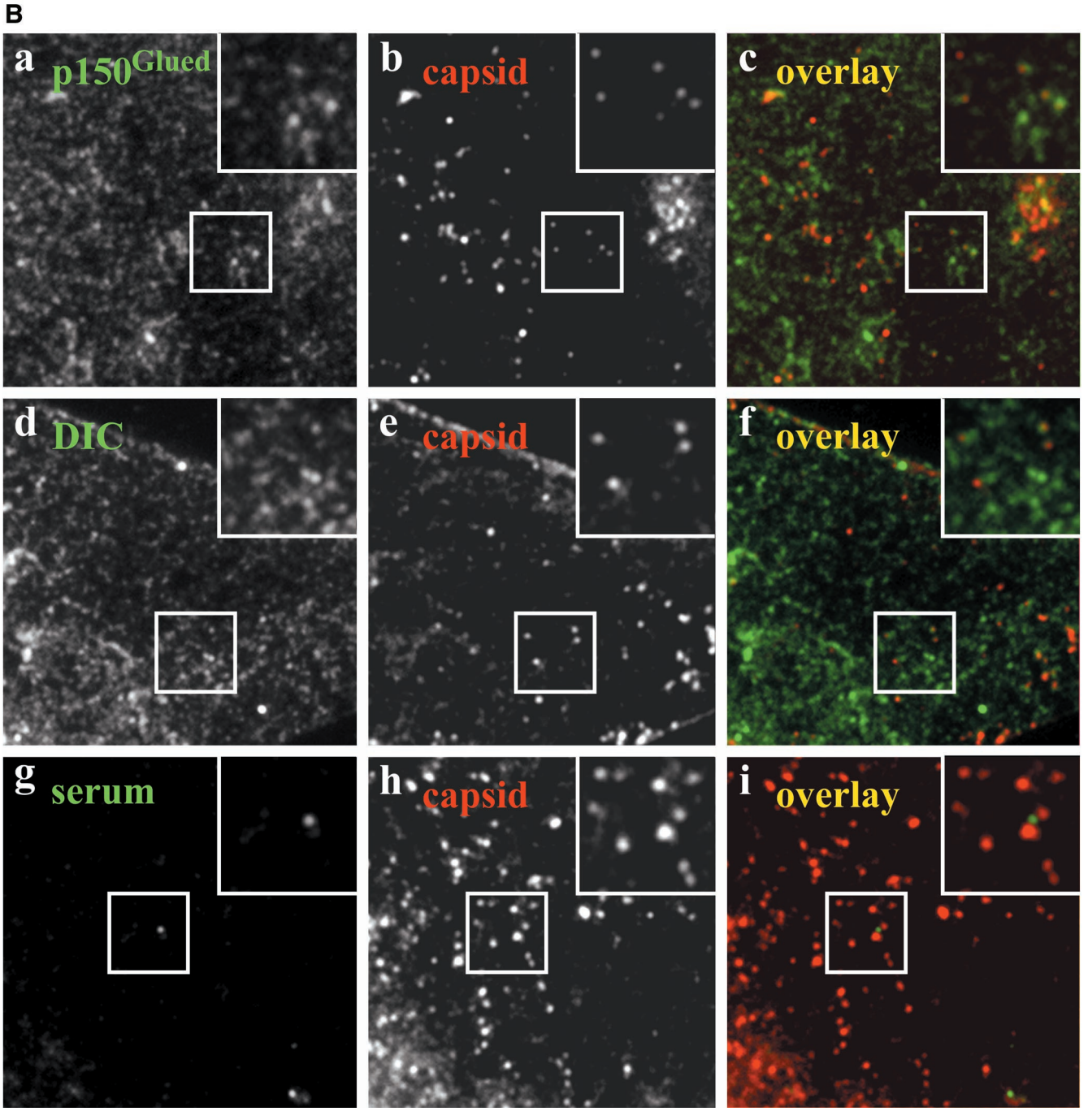

Figure 1 (legend on facing page).

All tegument proteins and the capsid with the DNA are released into the cytosol. In epithelial cells and in axons of cultured neuronal cells, incoming cytosolic capsids are transported along microtubules (MTs) to the nucleus (Kristensson *et al.*, 1986; Topp *et al.*, 1994; Topp *et al.*, 1996; Sodeik *et al.*, 1997). Electron microscopy and careful quantification demonstrated that ~70% of cytosolic capsids bind to nuclear pores and that concomitantly these capsids have lost their electron-dense core (Sodeik *et al.*, 1997). Using an in vitro uncoating assay, Ojala *et al.* (2000) demonstrated that capsid binding to the nucleus requires importin-β and that the release of the viral DNA is triggered by the interaction with the nuclear pore. Transcription, viral replication, and capsid assembly take place in

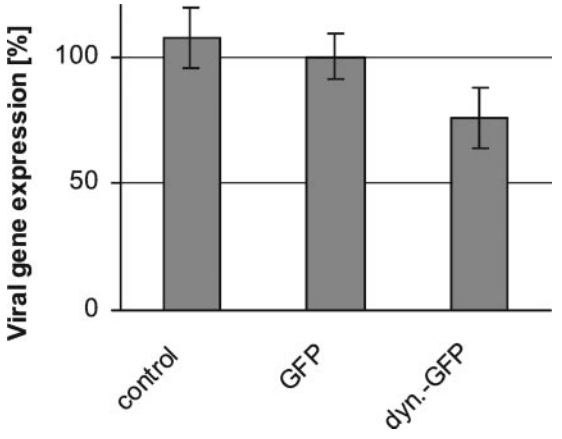

Figure 2. Quantification of immediate-early viral gene expression in transfected cells. β-Galactosidase activity per cell was reduced in dynamitin-GFP–overexpressing cells compared with untransfected or GFP-transfected cells. Two-sided Student's *t* test confirmed that viral protein synthesis is significantly lower in dynamitin-GFP–transfected cells compared with either GFP-transfected cells ($p = 1.13 \times 10^{-4}$) or to untransfected control cells ($p = 2.1 \times 10^{-5}$). There was no significant difference in β-galactosidase expression between control and GFP-transfected cells ($p = 1.58 \times 10^{-1}$). The mean values for five independent experiments each performed in duplicates are shown.

the nucleus (for reviews see Steven and Spear, 1997; Roizman and Knipe, 2001).

MTs are polar hollow protein cylinders of tubulin with a fast-growing and -shrinking plus end usually located toward the cell periphery and a minus-end mostly stabilized by attachment to the centrosome, the major microtubule organizing center (MTOC; Nogales, 2000). Most if not all minus-end–directed MT transport is mediated during interphase by dynein motors, whereas kinesins transport cargo toward the opposite direction (Vallee and Sheetz, 1996; Hirokawa, 1998). Cytoplasmic dynein is a 20 S MT-activated ATPase consisting of two dynein heavy chains (DHC), two intermediate chains (DIC), four light intermediate chains (DLIC) and four different classes of light chains (DLC; Karki and Holzbaur, 1999; King, 2000). Dynein is responsible for the perinuclear localization of several organelles around the MTOC and retrograde organelle transport in axons and is active during mitosis (Vallee and Sheetz, 1996; Hirokawa, 1998).

In many cases dynein is assisted by a second 20 S protein complex, called dynactin (Vallee and Sheetz, 1996; Karki and Holzbaur, 1999). It consists of 2 copies of $p150^{Glued}$, 4 molecules of dynamitin, p62, ~10 copies of Arp1 (actin-related-protein 1), possibly 1 conventional actin, Arp11, and actin capping protein (p37 and p32), p27, p25, and p24 (Holleran *et al.*, 1998; Eckley *et al.*, 1999). $p150^{Glued}$ can bind directly to DIC and thus link dynein to dynactin (Karki and Holzbaur, 1995; Vaughan and Vallee, 1995). Dynamitin, at high concentrations after transient transfection, dissociates the dynactin complex (Echeverri *et al.*, 1996; Eckley *et al.*, 1999). Excess dynamitin affects all tested dynein-mediated transports in vivo and in vitro: e.g., spindle organization, chromosome transport, and the subcellular localization of several membrane organelles (Echeverri *et al.*, 1996; Burkhardt *et al.*, 1997; Presley *et al.*, 1997; Valetti *et al.*, 1999; Sharp *et al.*, 2000).

Quantitative immunoelectron microscopy showed that DHC colocalizes with incoming herpes virus capsids (Sodeik *et al.*, 1997). Here, we demonstrate that incoming HSV1 capsids also colocalized with DIC and the $p150^{Glued}$ subunit of dynactin. To test whether HSV1 capsids use cytoplasmic dynein for their transport to the nucleus, we transiently transfected cells with dynamitin, subsequently challenged them with HSV1, and measured virus binding, internalization, capsid transport to the nucleus, and immediate-early viral gene expression. High concentrations of dynamitin and dynamitin-GFP clearly reduced the number of viral capsids transported to the nucleus compared with untransfected cells. Because fewer capsids reached the nucleus, presumably fewer viral genomes were delivered to the nucleoplasm, and the amount of viral protein synthesis was reduced. Overexpression of dynamitin did not downregulate virus receptors at the plasma membrane, because both virus binding and internalization were not reduced. We propose that incoming HSV1 capsids are propelled by dynein along MTs and that functional dynactin is required for their efficient transport.

MATERIALS AND METHODS

Cells and Antibodies

PtK_2 cells (ATCC CCL-56) were grown in 10%, Vero cells (ATCC CCL-81) in 7.5%, and BHK-21 cells (ATCC CCL-10) in 15% fetal calf serum. The media contained MEM, 2 mM glutamine, nonessential amino acids, and with the exception of the PtK_2 medium 100 U/ml penicillin and 100 μg/ml streptomycin.

Dynamitin expression was analyzed using mAb 50.1 (Paschal *et al.*, 1993) or a rabbit anti-myc antibody (Gee *et al.*, 1997), DHC was detected with affinity-purified rabbit pAb (Vaisberg *et al.*, 1993), DIC with a rabbit pAb L5 (Vaughan and Vallee, 1995), $p150^{Glued}$ with rabbit pAbs D'Artagnon, Aramis, or Portos (Vaughan and Vallee, 1995), and the cation-independent mannose-6-phosphate receptor with a rabbit pAb (Griffiths *et al.*, 1988). MTs were visualized using mouse mAb 1A2 (Kreis, 1987) and actin filaments with TRITC-Phalloidin (Sigma-Aldrich, Schnelldorf, Germany). We used preadsorbed rabbit pAbs raised against DNA-containing capsids (anti-HC) and empty capsids (anti-LC; Cohen *et al.*, 1980) and a mouse mAb 5C10 against VP5 (Newcomb *et al.*, 1996) to detect incoming viral capsids by immunofluorescence microscopy (Sodeik *et al.*, 1997). Immediate-early viral gene expression was measured with a mouse mAb against ICP4 (Showalter *et al.*, 1981). Viral glycoproteins were labeled with mouse mAb DL6 against gD and rabbit pAb R68 against gB (Eisenberg *et al.*, 1985, 1987). Secondary antibodies were purchased from Dianova (Hamburg, Germany).

Virological Techniques

Preparation of Stock Virus Cold and radioactively labeled virus stocks of HSV1 were prepared as described (Sodeik *et al.*, 1997). We used wild-type strain F (ATCC VR-733) and two HSV1 mutants: strain [KOS]tk12, which expresses the LacZ gene controlled by the immediate-early ICP4 promoter (Warner *et al.*, 1998) and strain R7202, which lacks the majority of the glycoprotein E codons including the start codon and therefore does not exhibit viral Fc receptor activity (Baines and Roizman, 1993).

Plaque Assay Virus was diluted in 10-fold steps in RPMI with 0.2% wt/vol BSA, 20 mM HEPES, pH 7.0 (RPMI/BSA) and incubated in six-well dishes with just-confluent Vero cells for 1 h at room tem-

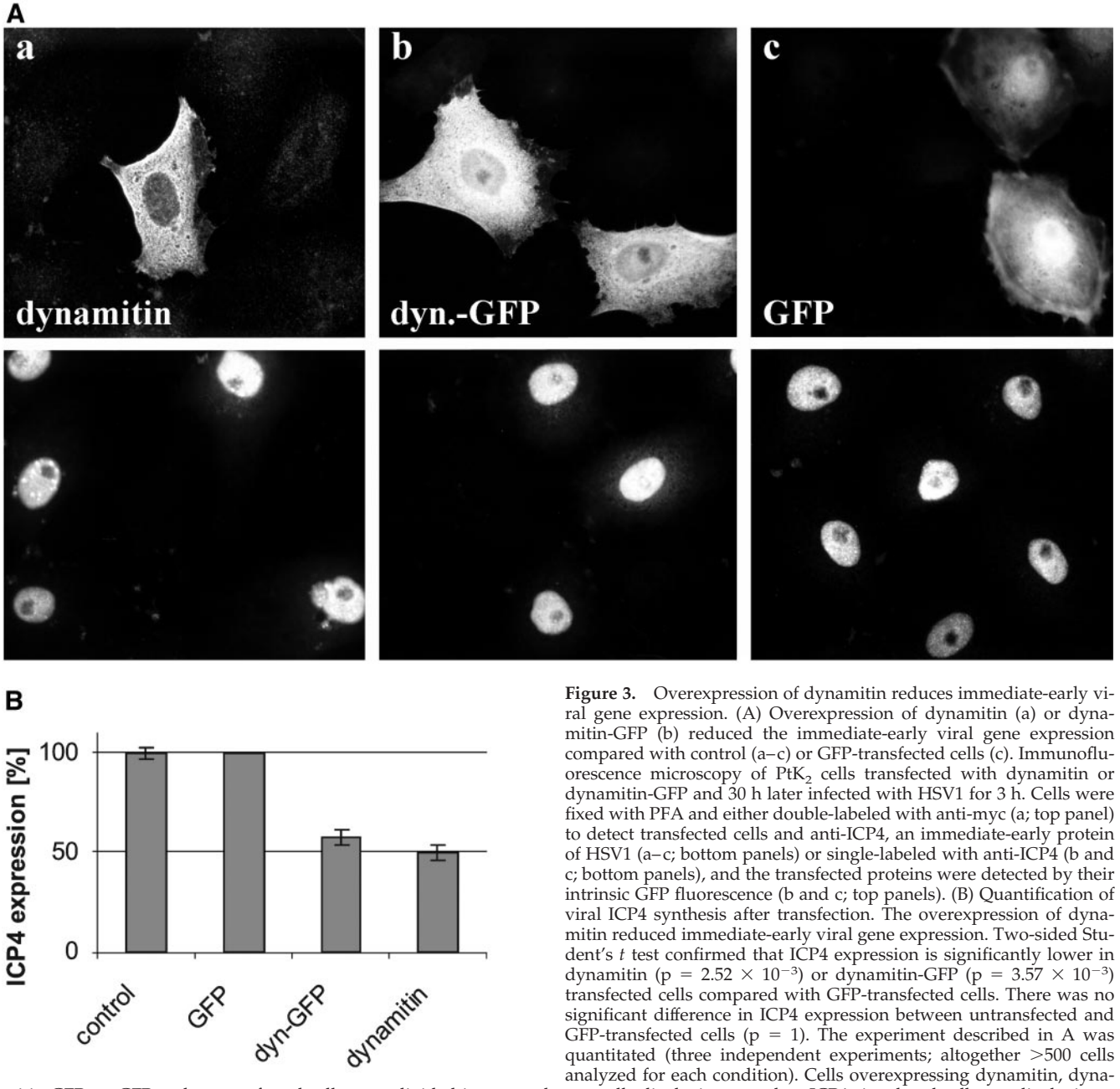

Figure 3. Overexpression of dynamitin reduces immediate-early viral gene expression. (A) Overexpression of dynamitin (a) or dynamitin-GFP (b) reduced the immediate-early viral gene expression compared with control (a–c) or GFP-transfected cells (c). Immunofluorescence microscopy of PtK_2 cells transfected with dynamitin or dynamitin-GFP and 30 h later infected with HSV1 for 3 h. Cells were fixed with PFA and either double-labeled with anti-myc (a; top panel) to detect transfected cells and anti-ICP4, an immediate-early protein of HSV1 (a–c; bottom panels) or single-labeled with anti-ICP4 (b and c; bottom panels), and the transfected proteins were detected by their intrinsic GFP fluorescence (b and c; top panels). (B) Quantification of viral ICP4 synthesis after transfection. The overexpression of dynamitin reduced immediate-early viral gene expression. Two-sided Student's *t* test confirmed that ICP4 expression is significantly lower in dynamitin ($p = 2.52 \times 10^{-3}$) or dynamitin-GFP ($p = 3.57 \times 10^{-3}$) transfected cells compared with GFP-transfected cells. There was no significant difference in ICP4 expression between untransfected and GFP-transfected cells ($p = 1$). The experiment described in A was quantitated (three independent experiments; altogether >500 cells analyzed for each condition). Cells overexpressing dynamitin, dynamitin-GFP, or GFP and untransfected cells were divided into two classes: cells displaying a nuclear ICP4 signal and cells not displaying a nuclear ICP4 signal.

perature on a rocking platform. The inoculum was removed, and 2 ml/well normal growth medium containing 10 μg/ml pooled human IgG (Sigma-Aldrich) was added. The cells were further cultured for 2 d at 37°C, 5% CO_2 and fixed in absolute methanol. After incubation with a mAb to gD (DL6) and a secondary anti-mouse antibody conjugated to alkaline phosphatase, the cells were washed with TSM (100 mM Tris-HCl, pH 9.5, 100 mM NaCl, 5 mM $MgCl_2$) and treated with 0.2 mM nitroblue tetrazolium chloride and 0.8 mM 5-bromo-4-chloro-3-indolyl phosphate until dark plaques became visible. We routinely obtained titers around 10^{10} PFU/ml for cold wild-type and HSV1[KOS]tk12 virus and 10^7 PFU/ml for ^{3}H-thymidine labeled virus.

Virus Infection Control and transfected Vero, BHK, or PtK_2 cells were inoculated with virus in RPMI/BSA for 2 h on ice to allow virus binding. After three washes with ice-cold RPMI/BSA, they were shifted to growth medium at 37°C and 5% CO_2. In those experiments analyzing the subcellular localization of incoming

viral particles, 0.5 mM cycloheximide was added to prevent synthesis of new viral proteins (Sodeik *et al.*, 1997). When nocodazole (50 μM) was used to depolymerize MTs, cells were pretreated for 1 h at 37°C, and the drug was present during all further incubation steps. For immunofluorescence microscopy in 24-well plates we used 8×10^6 PFU/well HSV1 for entry experiments, 1×10^7 PFU/well for virus binding experiments, and 4×10^5 PFU/well for ICP4 experiments.

Light Microscopy

Cells grown on coverslips were fixed with 3% (wt/vol) paraformaldehyde (PFA in PBS) for 20 min followed by 50 mM NH_4Cl/PBS for 10 min and 0.1% Triton X-100/PBS for 5 min. For colocalization studies and visualization of MTs, cells were fixed with PHEMO-fix (3.7% [wt/vol] PFA, 0.05% [wt/vol] glutaraldehyde, 0.5% Triton X-100 in PHEMO buffer) either at room temperature or at 37°C for 10 min, and washed with PHEMO buffer (68 mM PIPES, 25 mM HEPES, pH 6.9, 15 mM EGTA, 3 mM $MgCl_2$, 10% [vol/vol] DMSO) followed by 50 mM NH_4Cl/PBS for 10 min.

In most experiments we used 10% (vol/vol) goat serum with 5 mg/ml BSA as blocking reagent and performed the immunolabeling essentially as described (Sodeik *et al.*, 1997). For the experiments described in Figure 1 we used 0.2 mg/ml human immunoglobulins (IgGs, I4506; Sigma, Taufkirchen, Germany) with 5 mg/ml BSA to block nonspecific protein binding.

HSV1 carries in its envelope a Fc-receptor with strong affinity for human IgGs, decreasing affinity for rabbit, sheep, and goat and no affinity for murine IgGs (reviewed in Dubin *et al.*, 1992). The degree of the Fc-receptor–specific signal in the absence of human IgGs depended strongly on the protocol used: it was most prominent under the conditions we found optimal for the colocalization studies, namely after PHEMO fixation at room temperature, but surprisingly only weak after PHEMO fixation at 37°C or after PFA fixation followed by TX-100 (our unpublished results). Initial double-labeling experiments for dynein or dynactin with HSV1 capsids demonstrated that in the presence of human IgGs, primary rabbit and secondary goat antibodies bound only with their antigen-binding domain but not with their Fc-domain to infected cells. Without human IgGs, the membrane of incoming virions was also detected by preimmune and immune rabbit sera but not by unspecific mouse antibodies (our unpublished results).

The cells were examined with a fluorescence microscope (DM IRB/E; Leica, Wetzlar, Germany), and micrographs were taken on Kodak TMAX-400 (Eastman Kodak, Rochester, NY) or Ilford HP5 400 films (Ilford, Cheshire, United Kingdom). All digitized images (using a Nikon LS-1000 35-mm film scanner; Tokyo, Japan) were image processed using Adobe Photoshop version 5.5 (San Jose, CA). Colocalization and expression levels were analyzed using a digital interline charge coupled device camera (MicroMax-5MHz-782Y; Princeton Instruments Inc., Princeton, NJ) and the Metamorph software version 4.01 (Universal Imaging Corporation, West Chester, PA). Dynamitin-GFP and GFP-expressing cells were scored as high expressors (see Figure 8B) when their average gray values in the cytoplasm were above 400 (exposure time: 0.2 s) using the function "show region statistics" of the Metamorph software. Cells overexpressing dynamitin (mAb 50.1) were scored as high expressors when their average gray values in the cytoplasm were above 600 (exposure time: 0.5 s).

Transient Transfection

Plasmids For transient transfections we used the plasmids pEGFP-N1 (Clontech Laboratories Inc., Palo Alto, CA) expressing enhanced green fluorescent protein (GFP) and p50 expressing myc-tagged dynamitin (Echeverri *et al.*, 1996). For the dynamitin-GFP–expressing construct (p50-GFP), the full dynamitin cDNA sequence was inserted upstream of GFP into the pEGFP-N1 vector between the *Eco*RI and the *Bam*HI sites. The proper restriction sites were created by PCR, and subsequent products were sequenced to ensure that no mutation was created. All constructs are under the control of the cytomegalovirus immediate-early promotor (Clontech).

Experiments Measuring Virus Binding, Internalization, and Protein Synthesis PtK_2 cells were seeded in 10-cm diameter culture dishes at a density of 5×10^5. Twenty-four hours later the cells were transfected with 30 μg DNA per dish using calcium phosphate (Sambrook *et al.*, 1989). After 24 h, the cells were washed once with PBS, and 10 ml/dish normal growth medium was added for 19–22 h.

Experiments Analyzed by Immunofluorescence Microscopy Transfections were made with calcium phosphate or lipofectamine reagent (Life Technologies, Karlsruhe, Germany). For the latter, cells were seeded onto coverslips (12-mm diameter) in a 24-well cell culture dish at a density of 4×10^4 (Vero) or 3×10^4 (PtK_2) cells per well. After 16–18 h, the cells were washed twice with serum-free, antibiotic-free MEM and incubated with 300 μl/well serum-free, antibiotic-free MEM containing 1.5 μl/well lipofectamine and 150 ng DNA for 5 h. The transfection mixture was removed, and 1 ml/well normal growth medium was added for 24–28 h. For transfections with calcium phosphate, PtK_2 cells were seeded onto coverslips (12-mm diameter) in a 24-well cell culture dish at a density of 2×10^4 cells per well. After 24 h cells were transfected with 1.1 μg DNA per well. Twenty-four hours later 1 ml/well normal growth medium was added for 19–22 h.

Immediate-early Viral Gene Expression

Immediate-early viral gene expression was analyzed using the mutant HSV1(KOS)tk12, which expresses the bacterial LacZ gene coding for the enzyme β-galactosidase under the control of the immediate-early ICP4 promotor of HSV1 (Warner *et al.*, 1998). PtK_2 cells transfected for 44 h with dynamitin-GFP or GFP were inoculated with 2 ml per 10-cm dish RPMI/BSA containing $4–8 \times 10^6$ PFU of HSV1(KOS)tk12 for 2 h on ice and then shifted to 37°C for 3–4 h. The cells were harvested by trypsinization, and trypsin was immediately inhibited by adding trypsin inhibitor, and further protein synthesis by cycloheximide. Transfection efficiencies were determined by flow cytometry (FACSCalibur; Becton Dickinson, Heidelberg, Germany), cell densities by BCA assay (Pierce, Rockford, IL) after lysis in 1% SDS/PBS, and β-galactosidase activities after lysis in 0.5% TX-100/PBS with 1 mg/ml BSA and protease inhibitors using *O*-nitrophenyl-β-D-galactopyranoside as substrate. β-Galactosidase activity per cell was normalized to GFP-transfected cells.

Quantification of Virus Binding and Internalization

We assayed for virus binding and internalization essentially as described using a protease protection assay (Sodeik *et al.*, 1997). PtK_2 cells transfected for 44 h with dynamitin-GFP or GFP were inoculated with 2 ml per 10-cm dish RPMI/BSA containing ^{3}H-thymidine labeled HSV1 (5–10 kBq and 8×10^6 to 1.6×10^7 PFU). Cell-associated radioactivity—representing the amount of bound virions—was determined by scintillation counting. Virus binding was expressed as radioactivity per cell and normalized to GFP-transfected cells. To assay for virus internalization, ^{3}H-thymidine-labeled virus was bound to transfected cells at 4°C for 2 h. The cells were washed to remove unbound virus, shifted to 37°C for 30 min, transferred back to ice, and washed with ice-cold RPMI. Cell associated radioactivity after proteinase K treatment was determined by scintillation counting (Sodeik *et al.*, 1997). In these virus binding and internalization experiments, the transfection efficiencies were measured by flow cytometry and cell densities using a hemocytometer.

RESULTS

Colocalization of Incoming HSV1 Capsids with Cytoplasmic Dynein and Dynactin

We have shown previously by quantitative immune electron microscopy that in Vero cells incoming cytosolic HSV1 capsids colocalize with DHC (Sodeik *et al.*, 1997). Here, we used PtK_2 cells that are extremely flat in the periphery to analyze the subcellular distribution of HSV1 relative to dynein and dynactin. In uninfected cells, anti-DHC, anti-DIC, and anti $p150^{Glued}$ revealed a weak diffuse labeling throughout the cytoplasm that was strongest around the nucleus; moreover, centrosomes and numerous tubules and vesicles concentrated around the nucleus were labeled (our unpublished results). These structures might represent host organelles that use dynein for transport along MTs (Burkhardt *et al.*, 1997; Sodeik *et al.*, 1997; Harada *et al.*, 1998; Valetti *et al.*, 1999; Habermann *et al.*, 2001).

After 1 h of infection, a mouse mAb to the capsid protein VP5 labeled numerous small fluorescent spots that represented individual capsids distributed over the entire cytoplasm (Figure 1, A and B, b, e, and h). After 2 h and more so after 3 h, the majority of capsids had accumulated at the nucleus (see Figure 7). Numerous small dots of dynactin (Figure 1Ac), DHC (our unpublished results), and DIC (Figure 1Af) colocalized with viral capsids, whereas there was no colocalization after double labeling with the mouse anti-VP5 and a preimmune rabbit serum (Figure 1Ai).

HSV1 carries in its envelope the viral protein complex gE/gI that has a strong Fc-receptor binding activity for human IgGs, decreasing affinity for rabbit, sheep, and goat, but does not bind to murine IgGs (reviewed in Dubin *et al.*, 1992). However, none of eight mouse monoclonal antibodies generated against different subunits of dynein (DHC, DIC, DLC) or dynactin ($p150^{Glued}$, dynamitin) showed any colocalization with viral capsids despite testing several fixation and permeabilization protocols. In the presence of rabbit or goat sera, we therefore blocked the Fc-receptor with human IgGs (cf. MATERIALS AND METHODS). Moreover, we used the HSV1 mutant R7202, which is deleted for gE and does not contain a Fc-binding activity (Baines and Roizman, 1993). After 1 h of infection with R7202, numerous viral capsids were also labeled for dynactin and dynein, in the presence (Figure 1B) and also absence (our unpublished results) of human IgGs.

Approximately 15–20% of incoming capsids from wild-type HSV1 and the mutant R7202 were labeled with antibodies to dynactin (20% for $p150^{Glued}$; $n = 130$) and dynein (15% for DIC; $n = 100$). The lacking reactivity of monoclonal antibodies and the incomplete colocalization using polyclonal rabbit sera directed against dynein or dynactin subunits might suggest that there was steric hindrance and thus only limited epitope access in a putative ternary complex of capsids, dynein, and dynactin. Alternatively, it is possible that only a subset of viral capsids binds to dynein and/or dynactin at a given time point. Because most subunits of dynein and dynactin only exist in 20 S complexes and not as soluble proteins, these data showed that both protein complexes, dynein and dynactin, were at least transiently present on incoming viral capsids.

Immediate-early Viral Gene Expression after Overexpression of Dynamitin

To test whether functional dynein and dynactin were required during HSV1 entry, we transfected PtK_2 cells with dynamitin, which inhibits many dynein-mediated transport processes (Echeverri *et al.*, 1996; Burkhardt *et al.*, 1997; Presley *et al.*, 1997; Valetti *et al.*, 1999). In cells overexpressing dynamitin or dynamitin-GFP, mannose-6-phosphate receptor containing organelles were scattered over the entire cytoplasm rather than concentrated in the perinuclear region (our unpublished results), indicating that the function of dynein was disrupted (Burkhardt *et al.*, 1997; Valetti *et al.*, 1999). We routinely obtained transfection efficiencies of 65–75% for dynamitin-GFP and 70–85% for GFP as measured by flow cytometry (our unpublished results).

We next infected transfected PtK_2 cells with a HSV1 mutant expressing β-galactosidase under the control of an immediate-early HSV1 promoter (HSV1[KOS]tk12; Warner *et al.*, 1998), and the enzyme activity was quantified as an indicator for immediate-early viral gene expression. β-galactosidase activity was highest in untransfected cells and lowest in cells transfected with dynamitin-GFP (Figure 2). Overexpressing dynamitin-GFP reduced the amount of β-galactosidase by 25% compared with overexpression of GFP alone.

To analyze single cells, we infected PtK_2 cells with wild-type HSV1 and double-labeled them with antibodies to the transiently expressed proteins and ICP4, an immediate-early, nuclear herpes virus protein (Everett, 2000). After overexpression of dynamitin and dynamitin-GFP there were about half as many cells labeled for ICP4 compared with GFP expressing or untransfected cells (Figure 3, A and B). Thus, the expression of ICP4 and β-galactosidase, both under the control of the ICP4 promotor, were reduced after overexpressing dynamitin or dynamitin-GFP compared with controls. Inhibition of immediate-early viral gene expression might be due to changes in 1) the MT-network, 2) virus binding to the cell surface, 3) virus internalization, or 4) a reduced cytosolic transport of incoming capsids to the nucleus.

The Cytoskeleton after Transient Transfection

Dynactin contains conventional actin, Arp1 and Arp11 (Schafer *et al.*, 1994; Eckley *et al.*, 1999). We therefore tested whether dynamitin overexpression affected the actin cytoskeleton in PtK_2 cells but detected no changes in filamentous actin upon transfection (our unpublished results; Burkhardt *et al.*, 1997). The overexpression of dynamitin can affect the organization of MTs in fibroblastic cells (Burkhardt *et al.*, 1997; Quintyne *et al.*, 1999). Because nuclear targeting of capsids is MT dependent (Sodeik *et al.*, 1997), we analyzed the MT-network in PtK_2 cells by immunofluorescence microscopy. In many cells, the MTs emanated to the peripheral cytoplasm from one location in the perinuclear region that most likely represents the position of the MTOC or centrosome (arrows in Figure 4). However, there were also cells in which there were several MT organizing zones around the nucleus rather than a single, well-defined MTOC or in which MTs emanated more broadly from the nuclear surface (asterisks in Figure 4). The number of cells without an apparent MTOC increased after overexpression of dynamitin (a) or

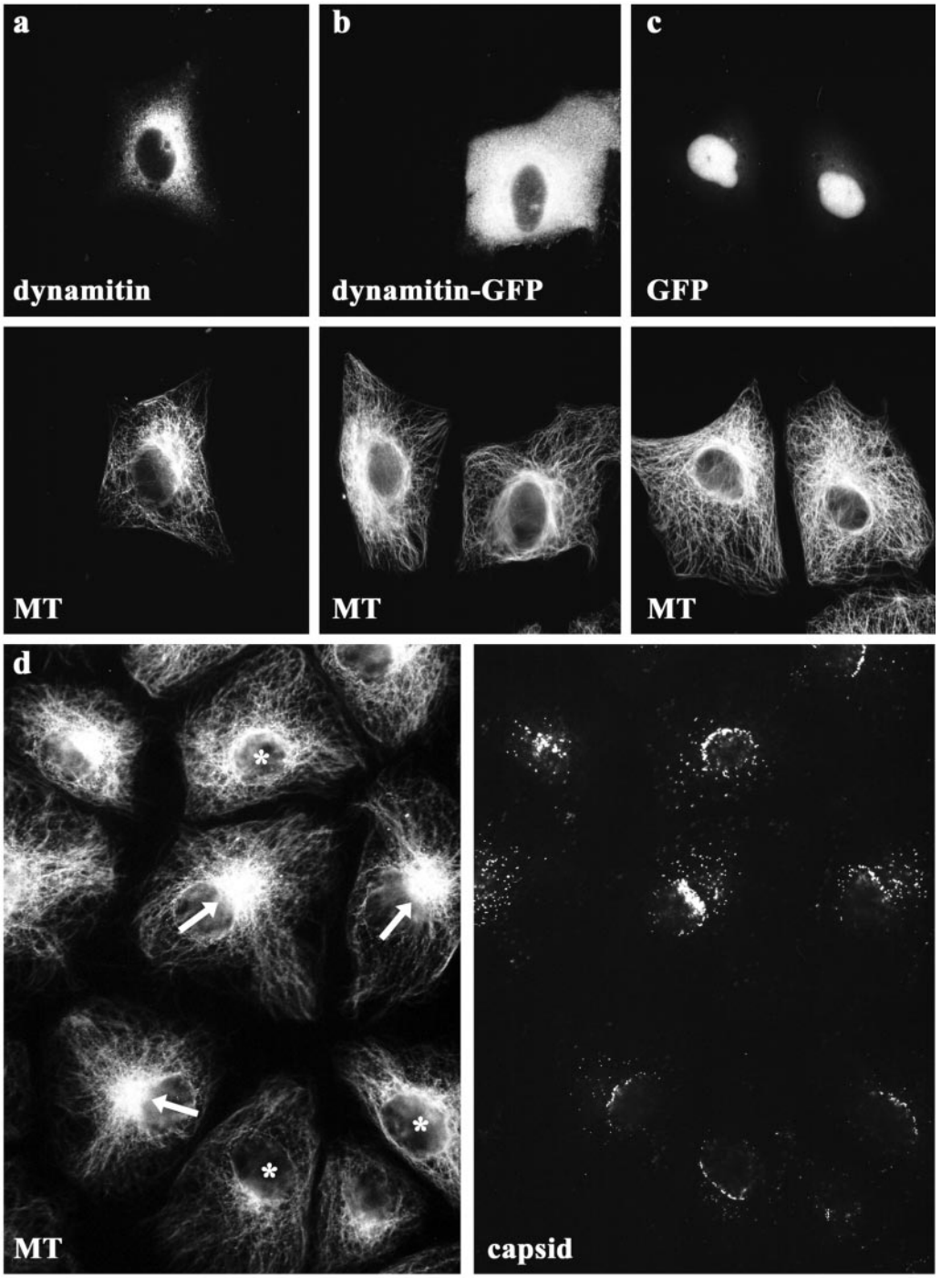

Figure 4. Organization of the microtubule network in transfected PtK_2 cells. Immunofluorescence microscopy showing the MT network of PtK_2 cells after overexpression of dynamitin or dynamitin-GFP. In almost all cells the MTs emanated from the perinuclear region of the cell. After overexpression of dynamitin (a) or dynamitin-GFP (b), there seemed to be fewer cells with a well-defined MTOC. In untransfected cells (b and d) and in cells overexpressing GFP (c), the MTs were focused at the MTOC in many cells. In untransfected cells with an apparent MTOC (arrows in d) and in cells with unfocussed MTs (asterisks in d) numerous capsids reached the nucleus (d, capsids). Twenty-eight hours after transfection, cells were fixed with PHEMO-fix and double-labeled with anti-myc (pAb, a; top panel) and anti-tubulin (mAb 1A2, a; bottom panel). Cells transfected with GFP proteins were only labeled with anti-tubulin (mAb 1A2, b and c; bottom panels). Note that because of the PHEMO-fixation, GFP was relocalized to the nucleus. In unfixed cells, most of the transiently expressed GFP was localized to the cytoplasm. In d, untransfected PtK_2 cells were infected with HSV1 for 3 h and fixed with PHEMO-fix at 37°C. Capsids were labeled with anti-LC (d; right panel) and MTs with 1A2 (d; left panel).

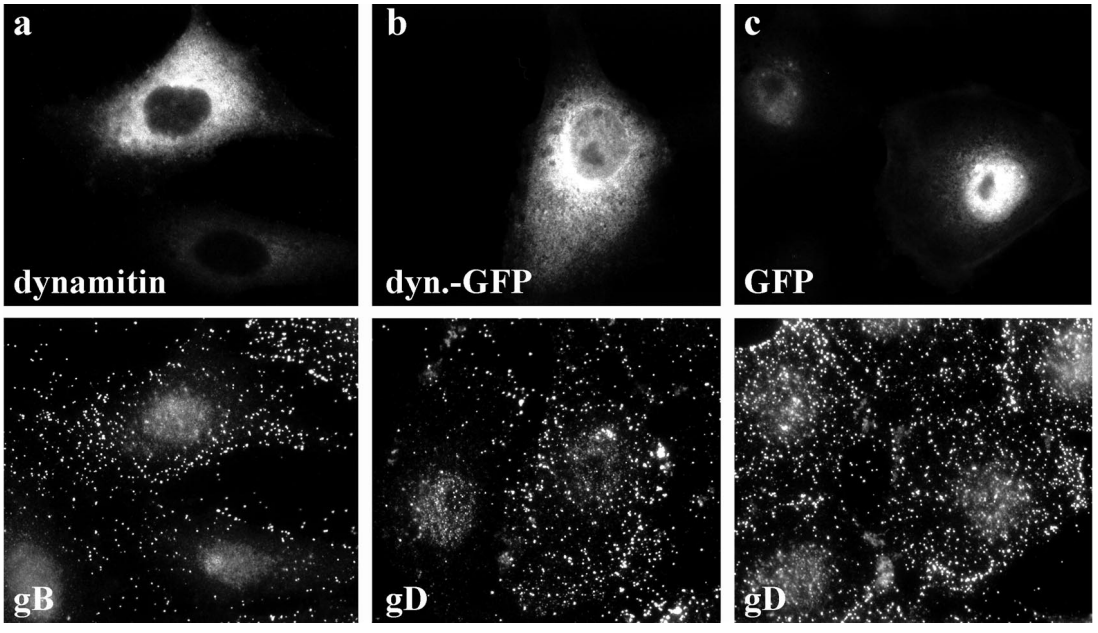

Figure 5. HSV1 binding and internalization in transfected cells. In cells overexpressing dynamitin (a) or dynamitin-GFP (b) virus binding was not reduced compared with untransfected cells or cells overexpressing GFP (c). Immunofluorescence microscopy of PtK_2 cells transfected with dynamitin or dynamitin-GFP and 20 h later inoculated with HSV1 for 2 h at 4°C. After 2 h at 4°C cells were washed and shifted to 37°C for 15 min to reduce unspecific binding, fixed in PFA and permeabilized with TX-100. They were double-labeled with anti-dynamitin (a; top panel) and anti-gB (a; bottom panel), and cells transfected with GFP proteins were only labeled with anti-gD (mAb DL6, b and c; bottom panels).

dynamitin-GFP (b), whereas GFP (c) did not have such an effect. However, also in untransfected cells without an obvious MTOC and unfocussed MTs many capsids reached the nucleus (Figure 4d, asterisks), suggesting that MTs but not focused MTs are required for nuclear targeting of HSV1 capsids.

Virus Binding and Internalization after Transfection

Overexpression of dynamitin affects both, secretory and endocytic membrane traffic (Burkhardt *et al.*, 1997; Presley *et al.*, 1997; Valetti *et al.*, 1999), and the concentration of HSV1 cell surface receptors present at the plasma membrane might therefore have been changed by the transfected proteins. Because several different molecules can serve as HSV receptors (Spear *et al.*, 2000), we decided to measure virus binding and internalization directly rather than trying to determine the subcellular localization of all potential viral surface receptors. To this end, cells overexpressing dynamitin, dynamitin-GFP, or GFP were infected with HSV1 for 15 min, fixed, and then labeled for the overexpressed proteins and viral glycoproteins. Compared with untransfected cells and with cells overexpressing GFP, glycoprotein labeling was unchanged by overexpression of dynamitin or dynamitin-GFP (Figure 5). Thus, the sum of surface-bound and internalized virus was similar under all conditions tested. Next we determined virus binding by measuring the amount of cell-bound virus and internalization using a protease protection assay (Sodeik *et al.*, 1997). After 2 h binding on ice ~50% of ^{3}H-thymidine–labeled HSV1 resist washing with buffer, and 95% of the bound virus can be detached from cells by proteinase treatment. If, however, the cells are warmed up, 70% of the bound HSV1 enters the cells with a half time of ~8 min (Sodeik *et al.*, 1997; our unpublished results).

Using these assays we determined that compared with untransfected or GFP-transfected PtK_2 cells, neither binding (Figure 6A) nor internalization (Figure 6B) of ^{3}H-thymidine–labeled HSV1 were reduced after overexpression of dynamitin-GFP. There seemed to be a slight increase of virus internalization in dynamitin-GFP– and GFP-transfected cells compared with control cells (Figure 6B). The reasons for that are unclear. However, the reduced viral protein synthesis after overexpression of dynamitin or dynamitin-GFP could neither result from reduced virus binding nor from reduced internalization.

Dynamitin Reduces Cytosolic Viral Capsid Transport to the Nucleus

The reduced amount of viral protein synthesis after overexpression of dynamitin could be due to impaired cytosolic transport of incoming capsids from the periphery to the nucleus. We therefore transiently transfected PtK_2 cells with dynamitin or dynamitin-GFP and infected them with HSV1 in the presence of cycloheximide.

Most capsids had reached the nucleus in untransfected cells as well as in cells overexpressing GFP 3 h after infection (Figure 7). In cells overexpressing dynamitin or dynamitin-GFP, fewer capsids were present at the nucleus. Interestingly, in many cells overexpressing dynamitin or dynamitin-

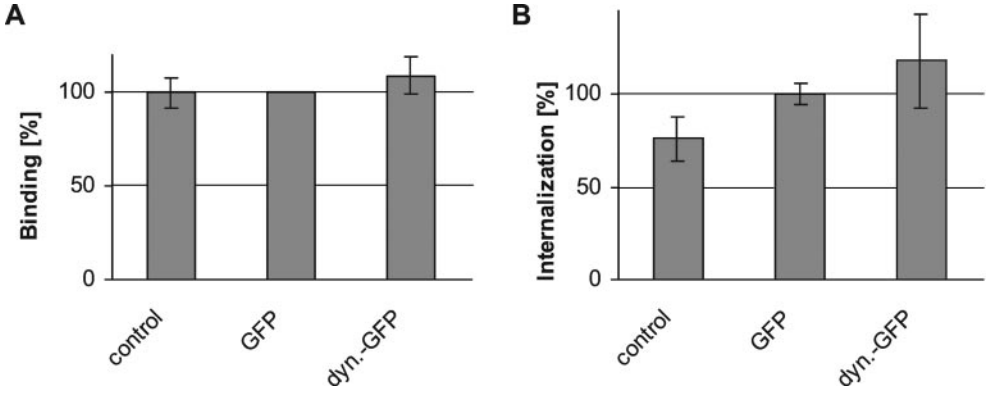

Figure 6. Quantification of HSV1 virus binding and internalization in transfected cells. (A) Virus binding after overexpression of dynamitin-GFP or GFP was identical to virus binding to mock-transfected cells (n = 2). Two-sided Student's *t* test confirmed that viral binding was not significantly different in dynamitin-GFP–transfected cells compared with either GFP-transfected cells ($p = 4.21 \times 10^{-1}$) or to untransfected control cells ($p = 4.03 \times 10^{-1}$). There was also no significant difference in viral binding between control and GFP-transfected cells ($p = 9.42 \times 10^{-1}$). Virus binding was calculated as radioactivity per cell and expressed as percent of radioactivity per cell compared with GFP-transfected cells. (B) Virus internalization after overexpression of dynamitin-GFP was not reduced compared with GFP-transfected cells (n = 6). Two-sided Student's *t* test confirmed that viral internalization was not significantly different in dynamitin-GFP–transfected cells compared with GFP-transfected cells ($p = 1.45 \times 10^{-1}$). However, compared with untransfected cells, virus internalization was higher in cells transfected with GFP ($p = 2.46 \times 10^{-3}$) or dynamitin-GFP ($p = 7.11 \times 10^{-3}$). Virus internalization was calculated as radioactivity per cell and expressed as percent of radioactivity per cell compared with GFP-transfected cells.

GFP the capsids were not randomly distributed over the entire cytoplasm as they are early in the infection (Sodeik *et al.*, 1997), but rather the capsids had accumulated in the cell margins (arrows in Figure 7, a and b). Similar results were obtained using BHK and Vero cells. However, BHK and Vero cells sometimes showed dramatic changes in cell morphology, whereas the morphology of PtK_2 cells was largely not affected by overexpressed dynamitin.

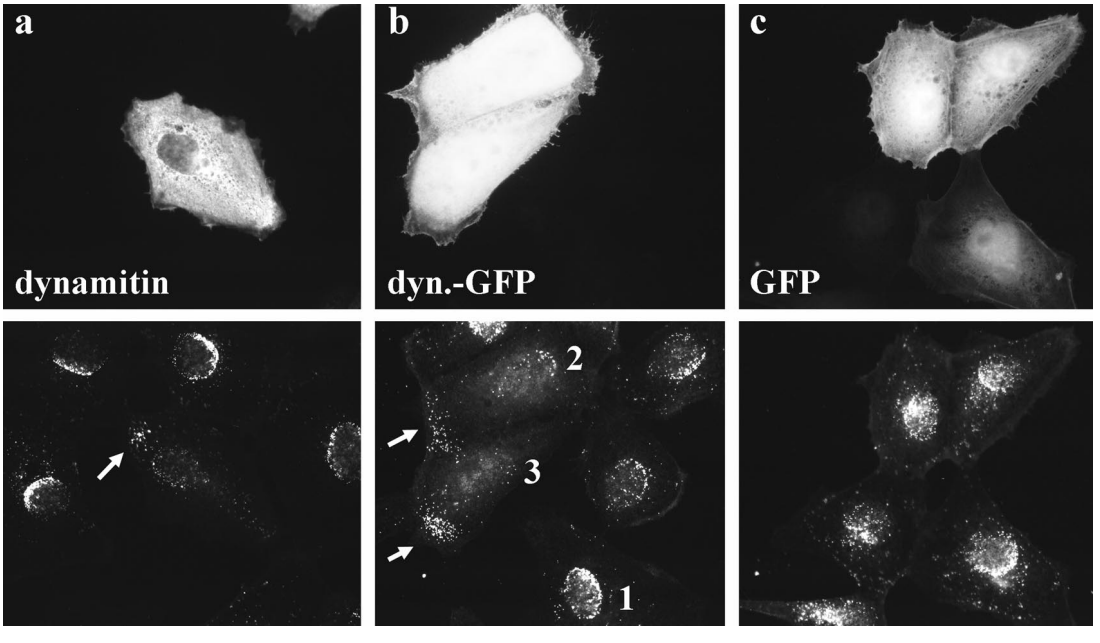

Figure 7. Overexpression of dynamitin reduces HSV1 capsid transport to the nucleus. Three hours after infection most capsids were bound to the nucleus in untransfected cells (a–c) and in cells overexpressing GFP (c). In cells overexpressing dynamitin (a) or dynamitin-GFP (b), only a few capsids reached the nucleus, and several capsids were seen in the periphery of the cells (arrows in a and b, bottom panels). Immunofluorescence microscopy of PtK_2 cells transfected with dynamitin or dynamitin-GFP and 46 h later infected with HSV1 for 3 h in the presence of cycloheximide. Cells were fixed with PFA, permeabilized with TX-100, and double-labeled with anti-dynamitin (mAb p50; a, top panel) and anti-HC (pAb; a, bottom panel). Cells transfected with GFP proteins were labeled with anti-HC (pAb; b and c, bottom panels).

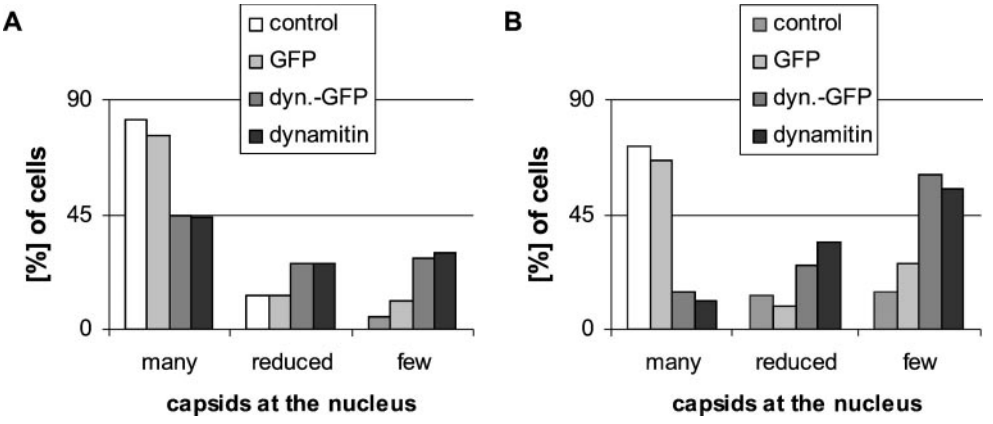

Figure 8. Quantification of viral capsid transport in transfected cells. For quantification, untransfected and transfected cells were randomly selected and classified into three different groups: cells with many capsids at the nucleus, typically forming a nuclear rim (Figure 7b, 1), cells with a reduced amount of capsids at the nucleus (Figure 7b, 2), and cells with <10 capsids at the nucleus (Figure 7b, 3). Either all (A) or only high expressing (B) cells were analyzed. Expression levels in the cytoplasm were determined using a digital camera. One can directly compare the expression levels for GFP with dynamitin-GFP (cf. MATERIALS AND METHODS). Dynamitin and dynamitin-GFP strongly inhibited HSV1 entry, whereas GFP had no effect on viral infection. Forty-five or 46 h after transfection with dynamitin, dynamitin-GFP, or GFP, PtK_2 cells were infected with HSV1 for 3 or 2 h (A and B, respectively), in the presence of cycloheximide. Cells were fixed with PFA, permeabilized with TX-100, and double-labeled with anti-capsid (anti-HC or anti-LC) and anti-dynamitin (cf. Figure 8). Cells with aggregated protein or abnormal morphology were excluded from analysis.

Occasionally, there seemed to be fewer capsids visible in cells overexpressing dynamitin or dynamitin-GFP than in control cells. This was due to the fact that in control cells most capsids were concentrated at the nuclear envelope and were thus visualized in one focus plane. In contrast in cells overexpressing dynamitin or dynamitin-GFP, capsids were distributed throughout the entire cytoplasm and therefore were not visualized in one focus plane. For quantification, PtK_2 cells were randomly selected and grouped into three different classes (cf. Figure 7b): 1) cells with many capsids at the nuclear envelope typically forming a nuclear crescent, 2) cells with a reduced amount of nuclear capsids, and 3) cells with very few capsids at the nucleus. The overexpression of dynamitin or dynamitin-GFP clearly reduced the number of cells that showed many capsids at the nucleus by ~50% compared with control or GFP-transfected cells (Figure 8A). Similar results were obtained using Vero cells overexpressing dynamitin (our unpublished results). As in other systems (Burkhardt *et al.*, 1997; Suomalainen *et al.*, 1999), we noticed that the degree of inhibition on capsid transport was dependent on the dose of the transfected protein. We therefore estimated expression levels using a digital camera and specifically analyzed cells expressing high amounts of the transfected proteins (Figure 8B). In these cells, dynamitin-GFP and dynamitin inhibited viral capsid transport by 85% compared with GFP-transfected or control cells.

At early time points, incoming capsids are distributed randomly over the entire cytoplasm (Sodeik *et al.*, 1997). However, in the cells in which the function of dynein was inhibited by the overexpression of dynamitin, the capsids were often concentrated in peripheral parts of the cells (Figure 9a). If dynamitin-transfected cells were infected in the presence of nocodazole, which disrupts the MT network, the capsids were also distributed randomly over the entire cytoplasm (Figure 9b). This experiment suggested that without the minus-end–directed MT motor dynein, the capsids might be transported by a plus-end–directed MT motor to the cell periphery.

In summary our data show that overexpressing dynamitin reduced the number of cytosolic viral capsids transported to the nucleus. Because under this condition fewer viral genomes reached the nucleoplasm, immediate-early viral gene expression was also reduced. The inhibition of virus entry by high amounts of dynamitin was not due to impaired virus binding, virus internalization, or the slight changes in the MT network but to a block of dynein function in cytosolic HSV1 capsid transport along MTs.

DISCUSSION

Incoming cytosolic HSV1 capsids are efficiently targeted along MTs from the plasma membrane to the nucleus (Hammonds *et al.*, 1996; Sodeik *et al.*, 1997; Mabit, Nakano, Prank, Saam, Döhner, Sodeik, Greber, unpublished data). The typical organization and polarity of MTs in cultured cells and axons require the use of a minus-end–directed MT motor for transport to the nucleus (Kristensson *et al.*, 1986; Topp *et al.*, 1994; Sodeik *et al.*, 1997; Bearer *et al.*, 2000). Cytoplasmic dynein is responsible for most minus-end–directed MT transport during interphase and thus a prime candidate for viral trafficking (Sodeik, 2000; Ploubidou and Way, 2001).

The dynein subunits DHC, DIC, and $p150^{Glued}$, a subunit of the dynein cofactor dynactin, colocalized with incoming HSV1 (Sodeik *et al.*, 1997; Figure 1). Moreover, EHNA (erythro-9–3-[2-hydroxynonyl]adenine), an inhibitor of axonemal and cytoplasmic dynein, blocks HSV1 infection in neuronal cells (Kristensson *et al.*, 1986). However, EHNA also affects adenosine deaminase, cGMP-stimulated phosphodiesterase, and the actin cytoskeleton (Penningroth, 1986; Mery *et al.*, 1995), and it is unclear which phase of the viral life cycle was inhibited. We therefore asked whether incoming HSV1 capsids use the host factor dynein for riding along MTs to the nucleus.

Inhibition of Dynein and Dynactin Does not Affect HSV1 Internalization

The function of dynactin and dynein can be inhibited by transiently overexpressing one dynactin subunit, the 50-kDa

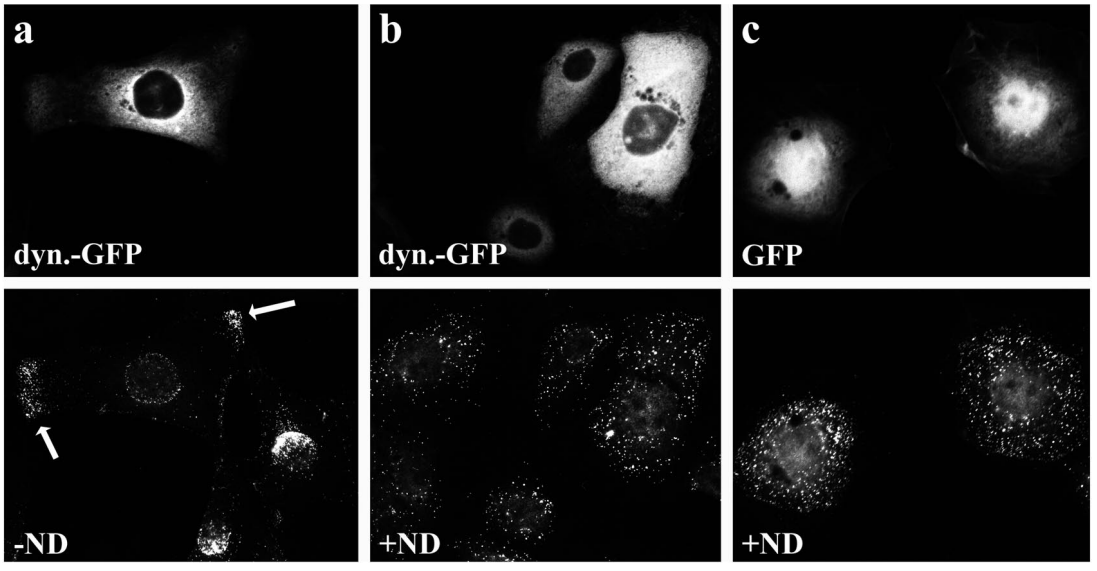

Figure 9. The peripheral accumulation in dynamitin expressing cells requires an intact MT network. In cells overexpressing dynamitin-GFP (a) or dynamitin, few incoming capsids reach the nucleus, and many accumulate in the peripheral cytoplasm 3 h after infection. If such cells are infected in the absence of MTs, incoming capsids are distributed randomly over the entire cytoplasm, and there is no peripheral accumulation (b). Immunofluorescence microscopy of PtK_2 cells transfected with dynamitin-GFP or GFP and 46 h later infected with HSV1 for 3 h in the presence of cycloheximide and in the absence (a) or presence (b and c) of nocodazole (ND). Cells were fixed with PFA, permeabilized with TX-100, and labeled with anti-VP5 (mAb 5C10; bottom panels).

protein dynamitin (Echeverri *et al.*, 1996). Because endocytic and exocytic membrane traffic involve dynein-mediated vesicular transport steps (Burkhardt *et al.*, 1997; Presley *et al.*, 1997; Valetti *et al.*, 1999), the subcellular localization of viral receptors might have been changed upon such treatment. However, none of the transfected proteins we tested reduced the efficiency of HSV1 binding or particle uptake. Thus, any influence on virus infection was not simply due to reduced surface expression of viral receptors and less efficient fusion of virions with the cells.

Inhibition of Dynein and Dynactin Blocks Cytosolic HSV1 Capsid Transport along MTs

Although virus entered transfected cells normally, overexpressed dynamitin inhibited the transport of cytosolic HSV1 capsids from the cell periphery to the nucleus by ~50% and in cells expressing high levels of dynamitin even by 85%. As a consequence viral immediate-early gene expression was reduced, too.

Two factors may have prevented a complete inhibition of virus infection in our set up. First, about a third of all cells were not transfected, and immunofluorescence microscopy confirmed that those were infected normally. Second, single cell analysis strongly suggested that the degree of capsid transport inhibition correlated with the level of dynamitin expression (Figure 8). This is consistent with biochemical experiments, which show that excess dynamitin blasts dynactin into two subcomplexes of 9 and 18 S, presumably by saturating dynamitin binding sites on them, thus destroying the architecture of dynactin (Echeverri *et al.*, 1996; Eckley *et al.*, 1999). Because this is likely to be a dose-dependent effect, it was expected that dynactin-dependent transport and virus infection were only completely inhibited in cells expressing high levels of dynamitin.

As in the absence of MTs (Sodeik *et al.*, 1997; Mabit, Nakano, Prank, Saam, Döhner, Sodeik, Greber, unpublished data), we detected a few capsids at the nuclear membrane in cells with high concentrations of dynamitin. This was no surprise, because virions can bind to the "apical" plasma membrane just on top of the nucleus. Capsids derived from these virions most likely reach the nuclear pores without MTs or dynein and dynactin. Dynein and dynactin–mediated MT transport is therefore not essential for infecting nonpolarized cells in culture. However, it is likely to be required during pathogenesis when HSV1 infects highly polarized epithelial and elongated neuronal cells (Enquist *et al.*, 1998), but also in less polarized cells, as described here, dynactin and the molecular motor dynein transport HSV1 capsids efficiently along MTs.

Functions of Dynein and Dynactin during HSV1 Capsid Transport?

ATP hydrolysis induces conformational changes in the DHC head domain, which produce a power stroke toward the MT minus end, whereas the smaller subunits DIC, DLIC, and DLC are attached to the stem domain (Habura *et al.*, 1999; Tynan *et al.*, 2000a), which is involved in cargo binding (Vaughan and Vallee, 1995; King, 2000; Tynan *et al.*, 2000b). Dynactin is needed for dynein-mediated vesicle transport (Gill *et al.*, 1991; Schroer and Sheetz, 1991) and transport of nonmembranous cargo such as NuMA aggregates, aggresomes, adenovirus capsids, neurofilaments, chromosomes, and pericentrin particles (Merdes and Cleveland, 1997; Gar-

cia-Mata *et al.*, 1999; Suomalainen *et al.*, 1999; Shah *et al.*, 2000; Sharp *et al.*, 2000; Young *et al.*, 2000).

Earlier electron microscopy data suggested that dynein binds with its stem domain to HSV1 capsids (Sodeik *et al.*, 1997). Our immunofluorescence microscopy data are consistent with either an indirect interaction via dynactin or a direct binding of HSV1 capsids to dynein. Dynactin might serve as an initial or permanent anchor for dynein on the capsid (Echeverri *et al.*, 1996) or tether between MT and capsid while dynein is detaching from the MT to make its next step (King and Schroer, 2000). The ATPase activity of dynein has also been reported to be regulated by dynactin-dependent phosphorylation (Kumar *et al.*, 2000).

Bidirectional HSV1 Capsid Transport along Microtubules?

Many subcellular structures and progeny GFP-tagged alphaherpes viruses (Smith *et al.*, 2001; Willard, 2002) can move bidirectionally along MTs. Interestingly, overexpression of dynamitin did not lead to a random capsid distribution but to their MT-mediated accumulation in the cell margins (Figures 7 and 9). This suggested that besides dynein, HSV1 capsids might also use a plus-end–directed MT motor. Plus-end–directed capsid motility could be involved in further transport from the MTOC to the nucleus, as would be required in cells where the MTOC is not directly neighboring the nucleus. MT-mediated, plus-end–directed capsid transport could also be involved in apical entry of polarized epithelial cells (Topp *et al.*, 1996). Moreover, during HSV1 egress from neurons, capsids are transported anterogradely to the presynapse (Miranda-Saksena *et al.*, 2000; Ohara *et al.*, 2000). Because of the uniform polarity of MTs in axons, this transport has to be catalyzed by a plus-end–directed motor.

If capsids were indeed able to travel along MTs in both directions, to the minus and plus ends, specific signals must regulate which motor the capsid is supposed to use during the different steps of the viral life cycle. Thus, the direction of capsid motility must be tightly controlled. The main transport direction during virus entry must be to MT minus-ends to ensure net movement to the cell center and the nucleus. However, if minus-end–directed, dynein-mediated transport was inhibited by overexpressing dynamitin, these putative plus-end–directed motors might have taken over and transported capsids to the cell margins.

Dynein or Kinesin Receptors Encoded by HSV1

In contrast to other cargo transported along MTs, the protein composition of HSV1 is known. There are ~20 tegument and capsid proteins that could function in motor or dynactin binding. The HSV1 gene product of UL34 interacts with DIC in GST pull down assays (Ye *et al.*, 2000). However, because UL34 has properties of a type-II membrane protein and in pseudorabies virus is not present in purified virions (Klupp *et al.*, 2000; Reynolds *et al.*, 2001), it remains to be seen how its interaction with DIC subunit could participate in viral capsid transport. The HSV1 tegument protein US11 was shown recently to interact with the heavy chain of conventional kinesin (Diefenbach *et al.*, 2002). Additional candidates for motor receptors include VP22 (UL49) and UL25, that both, upon transient transfection, seem to localize to MTs (Elliott and O'Hare, 1998; Kaelin *et al.*, 2000). In contrast to VP22 that dissociates from the capsid upon virus entry, UL25 and also VP1–3 (UL36) remain on the capsid until it reaches the nucleus (Morrison *et al.*, 1998; Kaelin *et al.*, 2000; Sodeik, Szmak and Prank, unpublished results).

Reconstitution of MT capsid motility in vitro (Wolfstein, Döhner, Allan and Sodeik, unpublished results) and HSV1 mutants can now be used to identify structural viral proteins required for capsid targeting to the nucleus.

ACKNOWLEDGMENTS

We thank Rudi Bauerfeind and Thomas F. Schulz (Hannover Medical School) for many helpful discussions and critical readings of the manuscript. We thank Bernard Roizman (University of Chicago, Chicago, IL) for providing the mutant strain R7202 and Patricia Spear (Northwestern University Medical School, Chicago, IL) for the mutant strain HSV[KOS]tk12. Doris Meder (Hannover Medical School) was instrumental in setting up the quantitative β-galactosidase assay in our laboratory. Melissa Gee, Kevin Vaughan (University of Massachusetts, Worcester, MA), Bernhard Hoflack (University of Lille, France), Roselyn Eisenberg, Gary Cohen (both at the University of Pennsylvania, Philadelphia, PA), Bill Newcomb, Jay Brown (both at the University of Virginia, Charlottesville, VA), Roger Everett (MRC Virology Unit, Glasgow, Scotland), and the late Thomas Kreis (University of Geneva, Switzerland) all graciously provided antibodies, and Jürgen Wehland (Gesellschaft für Biotechnologische Forschung, Braunschweig, Germany) the PtK_2 cells. K.D, A.W., U.P., and B.S. were supported by a grant from the Deutsche Forschungsgemeinschaft (So403/1), D.D by a fellowship from the Human Frontiers Science Program, and C.E., D.D. and R.V. by a National Institutes of Health (NIH) grant (GM 47434). Initial experiments for this study were performed at Yale University (New Haven, CT) and funded by an NIH grant to A.H. (AI 18599; now at the ETH, Zürich, Switzerland).

REFERENCES

Baines, J.D., and Roizman, B. (1993). The UL10 gene of herpes simplex virus 1 encodes a novel viral glycoprotein, gM, which is present in the virion and in the plasma membrane of infected cells. J. Virol. *67*, 1441–1452.

Bearer, E.L., Breakefield, X.O., Schuback, D., Reese, T.S., and LaVail, J.H. (2000). Retrograde axonal transport of herpes simplex virus: evidence for a single mechanism and a role for tegument. Proc. Natl. Acad. Sci. USA *97*, 8146–8150.

Burkhardt, J.K., Echeverri, C.J., Nilsson, T., and Vallee, R.B. (1997). Overexpression of the dynamitin (p50) subunit of the dynactin complex disrupts dynein-dependent maintenance of membrane organelle distribution. J. Cell Biol. *139*, 469–484.

Cohen, G.H., Ponce de Leon, M., Diggelmann, H., Lawrence, W.C., Vernon, S.K., and Eisenberg, R.J. (1980). Structural analysis of the capsid polypeptides of herpes simplex virus types 1 and 2. J. Virol. *34*, 521–531.

Diefenbach, R.J., Miranda-Saksena, M., Diefenbach, E., Holland, D.J., Boadle, R.A., Armati, P.J., and Cunningham, A.L. (2002). Herpes simplex virus tegument Protein US11 interacts with conventional kinesin heavy chain. J. Virol. *76*, 3282–3291.

Dubin, G., Fishman, N.O., Eisenberg, R.J., Cohen, G.H., and Friedman, H.M. (1992). The role of herpes simplex virus glycoproteins in immune evasion. Curr. Top. Microbiol. Immunol. *179*, 111–120.

Echeverri, C.J., Paschal, B.M., Vaughan, K.T., and Vallee, R.B. (1996). Molecular characterization of the 50-kD subunit of dynactin reveals function for the complex in chromosome alignment and spindle organization during mitosis. J. Cell Biol. *132*, 617–633.

Eckley, D.M., Gill, S.R., Melkonian, K.A., Bingham, J.B., Goodson, H.V., Heuser, J.E., and Schroer, T.A. (1999). Analysis of dynactin subcomplexes reveals a novel actin-related protein associated with the arp1 minifilament pointed end. J. Cell Biol. *147*, 307–320.

Eisenberg, R.J., *et al.* (1985). Localization of epitopes of herpes simplex virus type 1 glycoprotein D. J. Virol. *53*, 634–644.

Eisenberg, R.J., Ponce de Leon, M., Friedman, H.M., Fries, L.F., Frank, M.M., Hastings, J.C., and Cohen, G.H. (1987). Complement component C3b binds directly to purified glycoprotein C of herpes simplex virus types 1 and 2. Microb. Pathog. *3*, 423–435.

Elliott, G., and O'Hare, P. (1998). Herpes simplex virus type 1 tegument protein VP22 induces the stabilization and hyperacetylation of microtubules. J. Virol. *72*, 6448–6455.

Enquist, L.W., Husak, P.J., Banfield, B.W., and Smith, G.A. (1998). Infection and spread of alphaherpesviruses in the nervous system. Adv. Virus Res. *51*, 237–347.

Everett, R.D. (2000). ICP0, a regulator of herpes simplex virus during lytic and latent infection. Bioessays *22*, 761–770.

Garcia-Mata, R., Bebok, Z., Sorscher, E.J., and Sztul, E.S. (1999). Characterization and dynamics of aggresome formation by a cytosolic GFP-chimera. J. Cell Biol. *146*, 1239–1254.

Gee, M.A., Heuser, J.E., and Vallee, R.B. (1997). An extended microtubule-binding structure within the dynein motor domain. Nature *390*, 636–639.

Gill, S.R., Schroer, T.A., Szilak, I., Steuer, E.R., Sheetz, M.P., and Cleveland, D.W. (1991). Dynactin, a conserved, ubiquitously expressed component of an activator of vesicle motility mediated by cytoplasmic dynein. J. Cell Biol. *115*, 1639–1650.

Griffiths, G., Hoflack, B., Simons, K., Mellman, I., and Kornfeld, S. (1988). The mannose 6-phosphate receptor and the biogenesis of lysosomes. Cell *52*, 329–341.

Habermann, A., Schroer, T.A., Griffiths, G., and Burkhardt, J.K. (2001). Immunolocalization of cytoplasmic dynein and dynactin subunits in cultured macrophages: enrichment on early endocytic organelles. J. Cell Sci. *114*, 229–240.

Habura, A., Tikhonenko, I., Chisholm, R.L., and Koonce, M.P. (1999). Interaction mapping of a dynein heavy chain. Identification of dimerization and intermediate-chain binding domains. J. Biol. Chem. *274*, 15447–15453.

Hammonds, T.R., Denyer, S.P., Jackson, D.E., and Irving, W.L. (1996). Studies to show that with podophyllotoxin the early replicative stages of herpes simplex virus type 1 depend upon functional cytoplasmic microtubules. J. Med. Microbiol. *45*, 167–172.

Harada, A., Takei, Y., Kanai, Y., Tanaka, Y., Nonaka, S., and Hirokawa, N. (1998). Golgi vesiculation and lysosome dispersion in cells lacking cytoplasmic dynein. J. Cell Biol. *141*, 51–59.

Hirokawa, N. (1998). Kinesin and dynein superfamily proteins and the mechanism of organelle transport. Science *279*, 519–526.

Holleran, E.A., Karki, S., and Holzbaur, E.L. (1998). The role of the dynactin complex in intracellular motility. Int. Rev. Cytol. *182*, 69–109.

Kaelin, K., Dezelee, S., Masse, M.J., Bras, F., and Flamand, A. (2000). The UL25 protein of pseudorabies virus associates with capsids and localizes to the nucleus and to microtubules. J. Virol. *74*, 474–482.

Karki, S., and Holzbaur, E.L. (1995). Affinity chromatography demonstrates a direct binding between cytoplasmic dynein and the dynactin complex. J. Biol. Chem. *270*, 28806–28811.

Karki, S., and Holzbaur, E.L. (1999). Cytoplasmic dynein and dynactin in cell division and intracellular transport. Curr. Opin. Cell Biol. *11*, 45–53.

King, S.J., and Schroer, T.A. (2000). Dynactin increases the processivity of the cytoplasmic dynein motor. Nat. Cell Biol. *2*, 20–24.

King, S.M. (2000). The dynein microtubule motor. Biochim. Biophys. Acta *1496*, 60–75.

Klupp, B.G., Granzow, H., and Mettenleiter, T.C. (2000). Primary envelopment of pseudorabies virus at the nuclear membrane requires the UL34 gene product. J. Virol. *74*, 10063–10073.

Kreis, T.E. (1987). Microtubules containing detyrosinated tubulin are less dynamic. EMBO J. *6*, 2597–2606.

Kristensson, K., Lycke, E., Roytta, M., Svennerholm, B., and Vahlne, A. (1986). Neuritic transport of herpes simplex virus in rat sensory neurons in vitro. Effects of substances interacting with microtubular function and axonal flow [nocodazole, taxol and erythro-9–3-(2-hydroxynonyl)adenine]. J. Gen. Virol. *67*, 2023–2028.

Kumar, S., Lee, I.H., and Plamann, M. (2000). Cytoplasmic dynein ATPase activity is regulated by dynactin-dependent phosphorylation. J. Biol. Chem. *275*, 31798–31804.

Luby-Phelps, K. (2000). Cytoarchitecture and physical properties of cytoplasm: volume, viscosity, diffusion, intracellular surface area. Int. Rev. Cytol. *192*, 189–221.

Merdes, A., and Cleveland, D.W. (1997). Pathways of spindle pole formation: different mechanisms; conserved components. J. Cell Biol. *138*, 953–956.

Mery, P.F., Pavoine, C., Pecker, F., and Fischmeister, R. (1995). Erythro-9-(2-hydroxy-3-nonyl)adenine inhibits cyclic GMP-stimulated phosphodiesterase in isolated cardiac myocytes. Mol. Pharmacol. *48*, 121–130.

Miranda-Saksena, M., Armati, P., Boadle, R.A., Holland, D.J., and Cunningham, A.L. (2000). Anterograde transport of herpes simplex virus type 1 in cultured, dissociated human and rat dorsal root ganglion neurons. J. Virol. *74*, 1827–1839.

Morrison, E.E., Stevenson, A.J., Wang, Y.F., and Meredith, D.M. (1998). Differences in the intracellular localization and fate of herpes simplex virus tegument proteins early in the infection of Vero cells. J. Gen. Virol. *79*, 2517–2528.

Newcomb, W.W., Homa, F.L., Thomsen, D.R., Booy, F.P., Trus, B.L., Steven, A.C., Spencer, J.V., and Brown, J.C. (1996). Assembly of the herpes simplex virus capsid: characterization of intermediates observed during cell-free capsid formation. J. Mol. Biol. *263*, 432–446.

Nogales, E. (2000). Structural insights into microtubule function. Annu. Rev. Biochem. *69*, 277–302.

Ohara, P.T., Chin, M.S., and LaVail, J.H. (2000). The spread of herpes simplex virus type 1 from trigeminal neurons to the murine cornea: an immunoelectron microscopy study. J. Virol. *74*, 4776–4786.

Ojala, P.M., Sodeik, B., Ebersold, M.W., Kutay, U., and Helenius, A. (2000). Herpes simplex virus type 1 entry into host cells: reconstitution of capsid binding and uncoating at the nuclear pore complex in vitro. Mol. Cell. Biol. *20*, 4922–4931.

Paschal, B.M., Holzbaur, E.L., Pfister, K.K., Clark, S., Meyer, D.I., and Vallee, R.B. (1993). Characterization of a 50-kDa polypeptide in cytoplasmic dynein preparations reveals a complex with $p150^{Glued}$ and a novel actin. J. Biol. Chem. *268*, 15318–15323.

Penningroth, S.M. (1986). Erythro-9-[3-(2-hydroxynonyl)]adenine and vanadate as probes for microtubule-based cytoskeletal mechanochemistry. Methods Enzymol. *134*, 477–487.

Ploubidou, A., and Way, M. (2001). Viral transport and the cytoskeleton. Curr. Opin. Cell Biol. *13*, 97–105.

Presley, J.F., Cole, N.B., Schroer, T.A., Hirschberg, K., Zaal, K.J., and Lippincott-Schwartz, J. (1997). ER-to-Golgi transport visualized in living cells. Nature *389*, 81–85.

Quintyne, N.J., Gill, S.R., Eckley, D.M., Crego, C.L., Compton, D.A., and Schroer, T.A. (1999). Dynactin is required for microtubule anchoring at centrosomes. J. Cell Biol. *147*, 321–334.

Reynolds, A.E., Ryckman, B.J., Baines, J.D., Zhou, Y., Liang, L., and Roller, R.J. (2001). U(L)31 and U(L)34 proteins of herpes simplex virus type 1 form a complex that accumulates at the nuclear rim and is required for envelopment of nucleocapsids. J. Virol. *75*, 8803–8817.

Roizman, B., and Knipe, D.M. (2001). Herpes simplex viruses and their replication. In: Fundamental Virology, 4th ed., ed. B.N. Fields, D.M. Knipe, and P.M. Howley, *et al.,* Philadelphia: Lippincott-Raven Publishers, 2399–2459.

Sambrook, J., Fritsch, E.F., and Maniatis, T. (1989). Expression of cloned genes in cultured mammalian cells. In: Molecular Cloning: A Laboratory Manual, vol. 3, ed. C. Nolan, Cold Spring Harbor, NY: Cold Spring Harbor Laboratory Press.

Schafer, D.A., Gill, S.R., Cooper, J.A., Heuser, J.E., and Schroer, T.A. (1994). Ultrastructural analysis of the dynactin complex: an actin-related protein is a component of a filament that resembles F-actin. J. Cell Biol. *126*, 403–412.

Schroer, T.A., and Sheetz, M.P. (1991). Two activators of microtubule-based vesicle transport. J. Cell Biol. *115*, 1309–1318.

Shah, J.V., Flanagan, L.A., Janmey, P.A., and Leterrier, J.F. (2000). Bidirectional translocation of neurofilaments along microtubules mediated in part by dynein/dynactin. Mol. Biol. Cell *11*, 3495–3508.

Sharp, D.J., Rogers, G.C., and Scholey, J.M. (2000). Cytoplasmic dynein is required for poleward chromosome movement during mitosis in Drosophila embryos. Nat. Cell Biol. *2*, 922–930.

Showalter, S.D., Zweig, M., and Hampar, B. (1981). Monoclonal antibodies to herpes simplex virus type 1 proteins, including the immediate-early protein ICP 4. Infect. Immun. *34*, 684–692.

Smith, G.A., Gross, S.P., and Enquist, L.W. (2001). Herpesviruses use bidirectional fast-axonal transport to spread in sensory neurons. Proc. Natl. Acad. Sci. USA *98*, 3466–3470.

Sodeik, B. (2000). Mechanisms of viral transport in the cytoplasm. Trends Microbiol. *8*, 465–472.

Sodeik, B., Ebersold, M.W., and Helenius, A. (1997). Microtubule-mediated transport of incoming herpes simplex virus 1 capsids to the nucleus. J. Cell Biol. *136*, 1007–1021.

Spear, P.G., Eisenberg, R.J., and Cohen, G.H. (2000). Three classes of cell surface receptors for alphaherpesvirus entry. Virology *275*, 1–8.

Steven, A.C., and Spear, P.G. (1997). Herpesvirus capsid assembly and envelopment. In: Structural Biology of Viruses, ed. W. Chiu, R. Burnett, and R. Garcea, New York: Oxford University Press, 312–351.

Suomalainen, M., Nakano, M.Y., Keller, S., Boucke, K., Stidwill, R.P., and Greber, U.F. (1999). Microtubule-dependent plus- and minus end-directed motilities are competing processes for nuclear targeting of adenovirus. J. Cell Biol. *144*, 657–672.

Topp, K.S., Bisla, K., Saks, N.D., and Lavail, J.H. (1996). Centripetal transport of herpes simplex virus in human retinal pigment epithelial cells in vitro. Neuroscience *71*, 1133–1144.

Topp, K.S., Meade, L.B., and LaVail, J.H. (1994). Microtubule polarity in the peripheral processes of trigeminal ganglion cells: relevance for the retrograde transport of herpes simplex virus. J. Neurosci. *14*, 318–325.

Tynan, S.H., Gee, M.A., and Vallee, R.B. (2000a). Distinct but overlapping sites within the cytoplasmic dynein heavy chain for dimerization and for intermediate chain and light intermediate chain binding. J. Biol. Chem. *275*, 32769–32774.

Tynan, S.H., Purohit, A., Doxsey, S.J., and Vallee, R.B. (2000b). Light intermediate chain 1 defines a functional subfraction of cytoplasmic dynein which binds to pericentrin. J. Biol. Chem. *275*, 32763–32768.

Vaisberg, E.A., Koonce, M.P., and McIntosh, J.R. (1993). Cytoplasmic dynein plays a role in mammalian mitotic spindle formation. J. Cell Biol. *123*, 849–858.

Valetti, C., Wetzel, D.M., Schrader, M., Hasbani, M.J., Gill, S.R., Kreis, T.E., and Schroer, T.A. (1999). Role of dynactin in endocytic traffic: effects of dynamitin overexpression and colocalization with CLIP-170. Mol. Biol. Cell *10*, 4107–4120.

Vallee, R.B., and Sheetz, M.P. (1996). Targeting of motor proteins. Science *271*, 1539–1544.

Vaughan, K.T., and Vallee, R.B. (1995). Cytoplasmic dynein binds dynactin through a direct interaction between the intermediate chains and $p150^{Glued}$. J. Cell Biol. *131*, 1507–1516.

Wagner, E.K., and Bloom, D.C. (1997). Experimental investigation of herpes simplex virus latency. Clin. Microbiol. Rev. *10*, 419–443.

Warner, M.S., Geraghty, R.J., Martinez, W.M., Montgomery, R.I., Whitbeck, J.C., Xu, R., Eisenberg, R.J., Cohen, G.H., and Spear, P.G. (1998). A cell surface protein with herpesvirus entry activity (HveB) confers susceptibility to infection by mutants of herpes simplex virus type 1, herpes simplex virus type 2, and pseudorabies virus. Virology *246*, 179–189.

Whittaker, G.R., Kann, M., and Helenius, A. (2000). Viral entry into the nucleus. Annu. Rev. Cell Dev. Biol. *16*, 627–651.

Willard, M. (2002). Rapid directional translocations in virus replication. J. Virol. *76*, 5220–5232.

Ye, G.J., Vaughan, K.T., Vallee, R.B., and Roizman, B. (2000). The herpes simplex virus 1 U(L)34 protein interacts with a cytoplasmic dynein intermediate chain and targets nuclear membrane. J. Virol. *74*, 1355–1363.

Young, A., Dictenberg, J.B., Purohit, A., Tuft, R., and Doxsey, S.J. (2000). Cytoplasmic dynein-mediated assembly of pericentrin and gamma tubulin onto centrosomes. Mol. Biol. Cell *11*, 2047–2056.

Zhou, Z.H., Dougherty, M., Jakana, J., He, J., Rixon, F.J., and Chiu, W. (2000). Seeing the herpesvirus capsid at 8.5 A. Science *288*, 877–880.